Sensors and Materials, Vol. 37, No. 6 (2025) 2501–2506
MYU Tokyo

S & M 4069

Microstructure and Electrical Characteristics of NbMoTaW Thin Films

Cheng-Hsing Hsu,[1*] Yu-Hao Hsu,[1] and Chuan-Feng Shih[2]

[1]Department of Electrical Engineering, National United University,
No. 2 Lien-Da, Nan-Shih Li, Miao-Li 360302, Taiwan
[2]Department of Electrical Engineering, National Cheng-Kung University,
No. 1 University Road, Tainan 701401, Taiwan

(Received January 5, 2025; accepted May 19, 2025)

Keywords: high-entropy alloy, RF magnetron sputtering, electrical properties

We investigated the electrical properties and microstructures of high-entropy alloy NbMoTaW thin films prepared by radio frequency (RF) magnetron sputtering at different RF powers and substrate temperatures. Diffraction patterns indicated that the deposited films had a polycrystalline microstructure, and scanning electron microscopy results revealed that grain size was dependent on RF power and substrate temperature. The effects of processing parameters on the microstructure and electrical characteristics of the films were also investigated. The NbMoTaW alloy films are suitable for use as an electrode in sensors.

1. Introduction

Researchers have increasingly used high-entropy alloys with more than four elements for their adjustability and high hardness.[1,2] The favorable mechanical properties of these alloys are related to the formation of stable solid solutions.[3–9] Studies have demonstrated that the conductive properties of high-entropy alloys can be improved by screening for the appropriate metal elements to include in the alloys and by adjusting the processing parameters to reduce lattice defects in the alloys.[10–12] According to a previous study, the resistivity of a film based on the quaternary alloy NbMoTaW prepared by DC sputtering was approximately 170 μΩ-cm, similar to that of a conventional nickel-chromium alloy.[12] Therefore, this alloy can be used for electrodes in sensing components.[13]

In this study, radio frequency (RF) magnetron sputtering was used to produce high-entropy NbMoTaW alloy films on silicon substrates by using different substrate temperatures and RF powers. We investigated the deposition conditions affecting the physical and electrical properties of high-entropy NbMoTaW alloy films, and evaluated the applicability of sich films for use as an electrode in sensing components.

*Corresponding author: e-mail: hsuch@nuu.edu.tw
https://doi.org/10.18494/SAM5559

ISSN 0914-4935
https://myukk.org/

2. Experimental Procedures

RF magnetron sputtering was used to prepare high-entropy NbMoTaW alloy conducting thin films on Si substrates. A RF magnetron sputtering system with a fixed working pressure of 5 mTorr was used, and the films were prepared under different RF powers (100 and 200 W) and substrate temperatures (room temperature, 100, 200, and 300 °C). An X-ray diffractometer was used to analyze the composition of the films and determine changes in their crystal structure. An electron microscope was used to observe the surface morphology and thickness of the films, and the findings were used to determine the crystallization of the films. Finally, the four-point probe method was used to measure the resistivity of the films.

3. Results and Discussion

Figure 1 shows energy-dispersive X-ray spectroscopy (EDS) results indicating the films composition. According to these results, the relative content of each major element in the deposited films was maintained at 35%, which was consistent with the composition ratio of the target material.

Figure 2 shows the X-ray diffraction patterns of NbMoTaW films under different substrate temperatures and RF powers. The films' surface morphology and structural changes were observed by varying the RF power (100 or 200 W) and temperature. At the higher RF power, the incident ions bombarding the target had greater kinetic energy; this increased the overall sputtering efficiency and caused more particles to be deposited on the substrate surface to form a thin film. This also allowed for improved crystallinity and larger grain size in the entire film.

Element	Weight%	Atomic%
Si K	7.23	27.62
Nb L	13.88	16.01
Mo L	18.83	21.04
Ta M	32.20	19.08
W M	27.86	16.25
Totals	100.00	

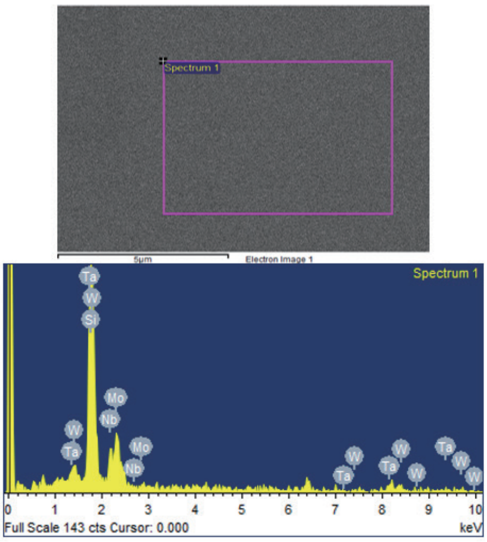

Fig. 1. (Color online) EDS data of NbMoTaW films at a power of 200 W and a substrate temperature of 300 °C.

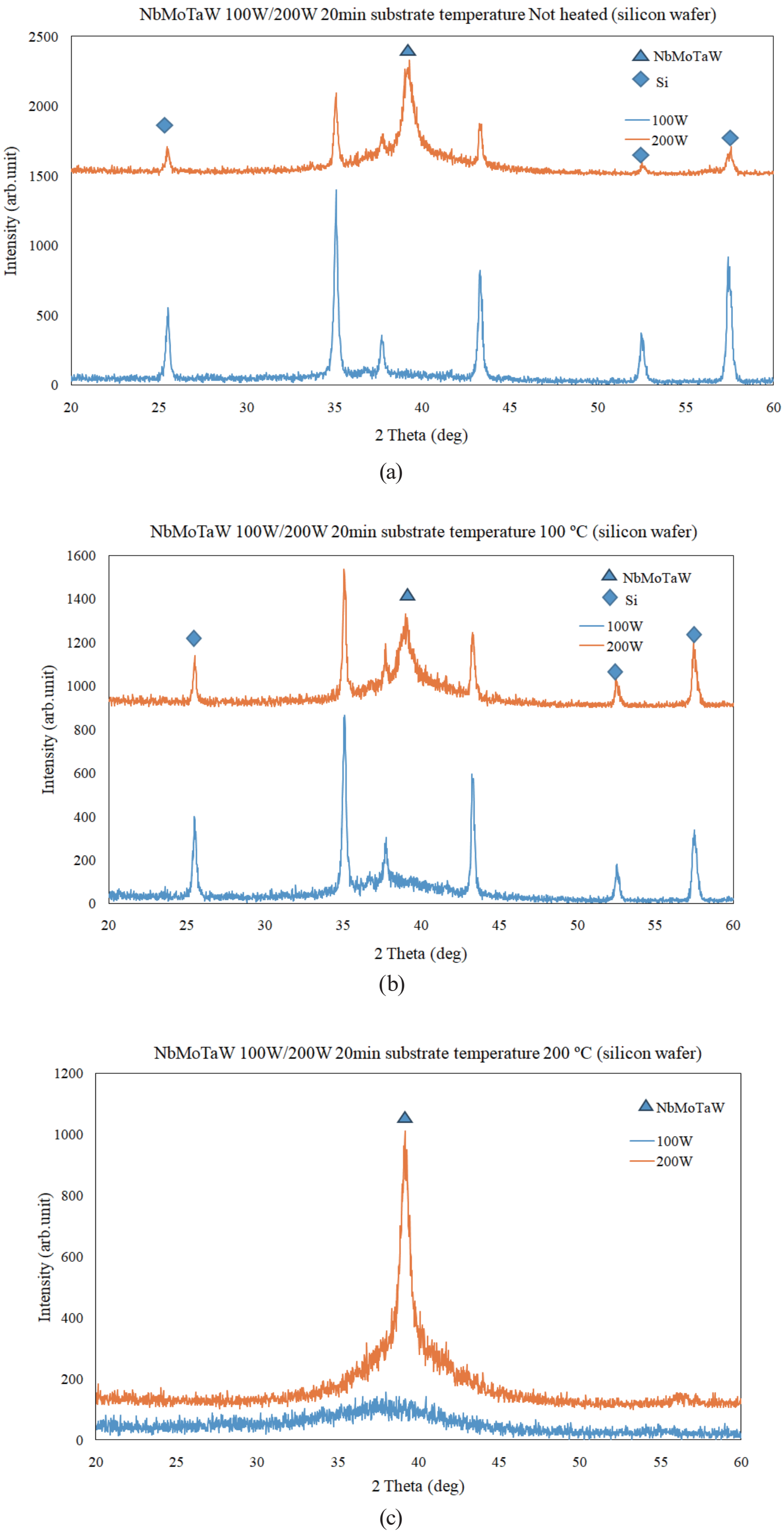

Fig. 2. (Color online) X-ray diffraction patterns of NbMoTaW films at various RF powers and substrate temperatures.

Figure 3 shows the SEM images of the surface structure of the NbMoTaW films under different substrate temperatures and an RF power of 200 W. The films had a texture akin to that of a wood leaf at a substrate temperature of 300 ℃. This notable microstructural change was likely due to quicker particle diffusion on the substrate surface when the substrate was heated during film growth. This heating promotes grain nucleation and growth. When the substrate was heated to 300 ℃, the surface structure changed because of the increase in energy on the substrate surface. When the substrate reaches a sufficiently high temperature, the energy on the substrate surface causes grain growth or reordering as particles from the target are deposited onto the substrate surface to form a thin film.

Figure 4 shows cross-sectional SEM images of high-entropy NbMoTaW alloy films under different substrate temperatures with a sputtering power of 200 W. According to these images, the films became thinner at higher substrate temperatures.

As illustrated in Fig. 5, resistivity was optimal (58 μΩ-cm) at a substrate temperature of 300 ℃ and an RF power of 200 W. This excellent resistivity performance can be attributed to this study's precise control of RF power, which increased the sputtering rate and provided more energy for particle crystallization. Although the change in substrate temperature is limited by the lattice effect of high-entropy alloys, resulting in poor thermal conductivity, a sufficiently high substrate temperature can still provide more kinetic energy to the particles and promote nucleation and crystallization.

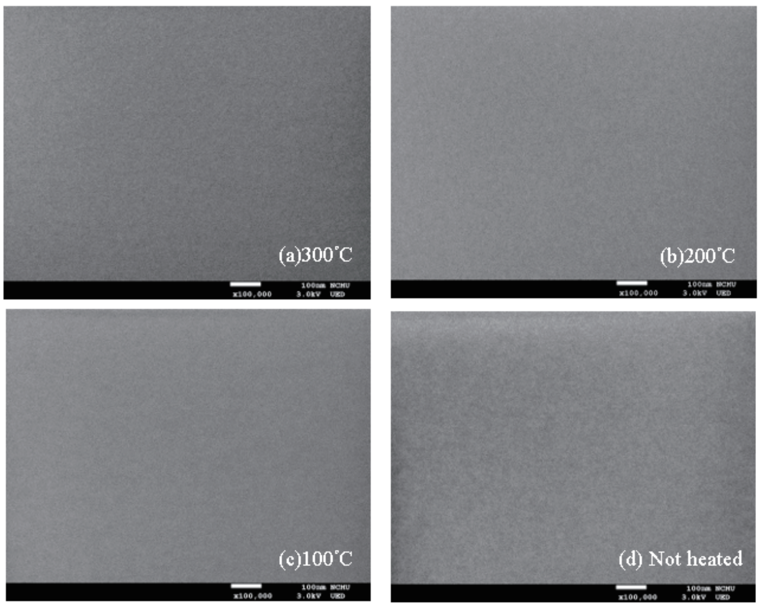

Fig. 3. SEM images of NbMoTaW films at an RF power of 200 W and various substrate temperatures.

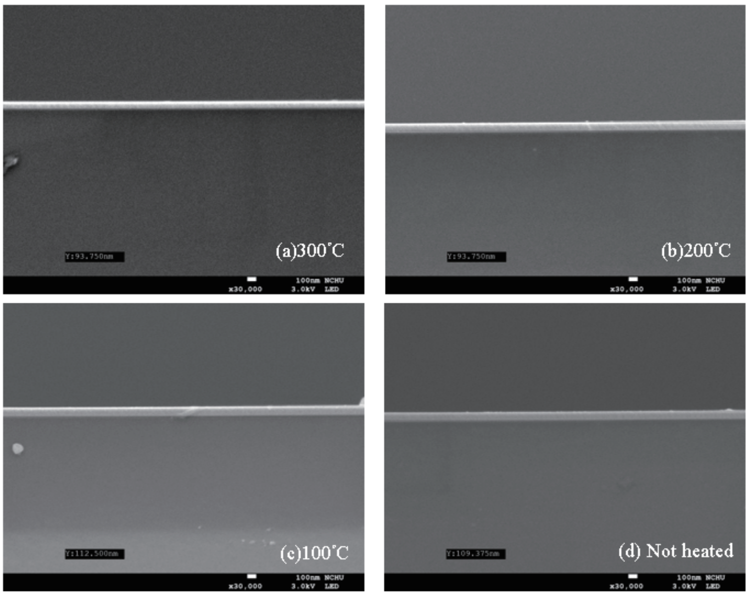

Fig. 4. Cross-sectional SEM images of NbMoTaW films at an RF power of 200 W at various substrate temperatures.

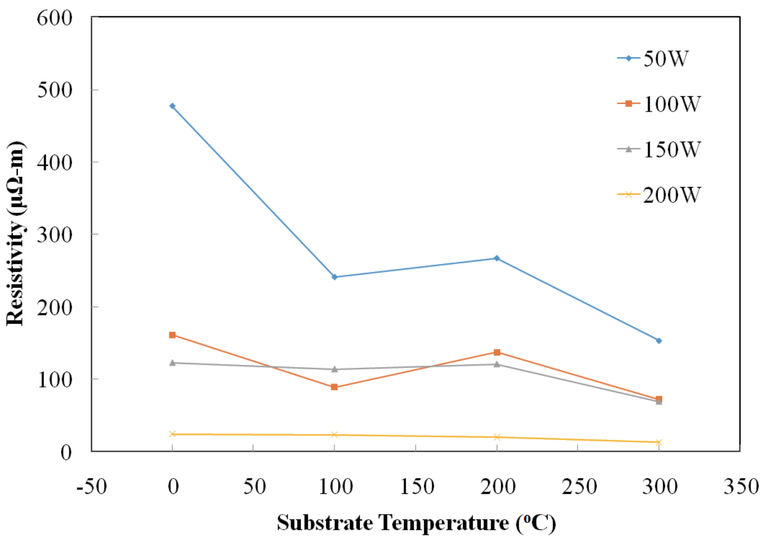

Fig. 5. (Color online) Resistivity of NbMoTaW thin films at various RF powers and substrate temperatures.

4. Conclusions

In this experimental study, we prepared high-entropy NbMoTaW alloy films on silicon substrates by RF magnetron sputtering. The physical properties and conductivity characteristics of these films were analyzed at different substrate temperatures and RF powers. The films' surface morphology and structural characteristics varied with deposition conditions, and the findings elucidated the growth mechanism and microstructural evolution of high-entropy alloy films. Resistivity was optimal (58 μΩ-cm) at a substrate temperature of 300 °C and an RF power of 200 W. These films can thus be used as electrodes in sensing elements.

Acknowledgments

This work was supported by the National Science and Technology Council of the Republic of China under grants nos. MOST 109-2622-E-239-005, NSTC 112-2221-E-239-015, NSTC 112-2224-E-006-004, and NSTC 113-2224-E-006 -001.

References

1 M. A. A. Hasan, J. Q. Wang, S. H. Shin, D. A. Gilbert, P. K. Liaw, N. Tang, W. L. N. C. Liyanage, L. Santodonato, L. DeBeer-Schmitt, and N. P. Butch: J. Alloys Compd. **883** (2021) 160811. https://doi.org/10.1016/j.jallcom.2021.160811
2 J. W. Yeh, S. K. Chen, S. J. Lin, J. Y. Gan, T. S. Chin, T. T. Shun, C. H. Tsau, and S. Y. Chang: Adv. Eng. Mater. **6** (2004) 299. https://doi.org/10.1002/adem.200300567
3 Y. Zhang, T. T. Zuo, Z. Tang, M. C. Gao, K. A. Dahmen, P. K. Liaw, and Z. P. Lu: Prog. Mater. Sci. **61** (2014) 1. https://doi.org/10.1016/j.pmatsci.2013.10.001
4 B. Gludovatz, A. Hohenwarter, D. Catoor, E. H. Chang, E. P. George, and R. O. Ritchie: Science **345** (2014) 1153. https://doi.org/10.1126/science.1254581
5 D. B. Miracle, J. D. Miller, O. N. Senkov, C. Woodward, M. D. Uchic, and J. Tiley: Entropy **16** (2014) 494. https://doi.org/10.3390/e16010494
6 K. Y. Tsai, M. H. Tsai, and J. W. Yeh: Acta Mater. **61** (2013) 4887. https://doi.org/10.1016/j.actamat.2013.04.058
7 C. W. Lin, M. H. Tsai, C. W. Tsai, J. W. Yeh, and S. K. Chen: Mater. Sci. Technol. **31** (2015) 1165. https://doi.org/10.1179/1743284715Y.0000000025
8 R. B. Nair, H. S. Arora, S. Mukherjee, S. Singh, H. Singh, and H. S. Grewal: Ultrason. Sonochem. **41** (2018) 252. https://doi.org/10.1016/j.ultsonch.2017.09.044
9 H. T. Zong, C. C. Geng, C. Y. Kang, G. H. Cao, L. Y. Bian, L. X. Li, B. Q. Zhang, and M. Li: Results Phys. **8** (2018) 253. https://doi.org/10.1016/j.rinp.2017.12.002
10 D. B. Miracle and O. N. Senkov: Acta Mater. **122** (2017) 448. https://doi.org/10.1016/j.actamat.2016.08.081
11 X. B. Feng, J. Y. Zhang, Z. R. Xia, W. Fu, K. Wu G. Liu, and J. Sun: Mater. Lett. **210** (2018) 84. https://doi.org/10.1016/j.matlet.2017.08.129
12 H. U. Kim, S. J. Nam, A. Roh, M. W. Son, M. H. Ham, J. H. Kim, and H. J. Choi: Int. J. Refract. Met. Hard Mater. **80** (2019) 286. https://doi.org/10.1016/j.ijrmhm.2019.02.005
13 C. H. Yeh, W. D. Hsu, B. H. Liu, C. S. Yang, C Y. Kuan, Y. C. Chang, K. S. Huang, S. S. Jhang, C. Y. Lu, P. K. Liaw, and C. F. Shih: Nat. Commun. **15** (2024) 4554. https://doi.org/10.1038/s41467-024-49035-0